Vietnam Journal of Science and Technology ***60*** *(4) (2022) 641-651*

doi:10.15625/2525-2518/16090

SERS CHEMICAL ENHANCEMENT OF 2,4,5-TRICHLOROPHENOXYACETIC ACID ABSORBED ON Au_{20}, ITS Au-Ag AND Au-Cu BIMETALLIC CLUSTERS: A DFT STUDY

Thi Thuy Huong Le[1, 2], Dinh Hieu Truong[3, 4], Thi Le Anh Nguyen[3, 4], Pham Minh Quan[1], Thi Chinh Ngo[3, 4], Duy Quang Dao[3, 4, *]

[1]*Institute of Natural Products Chemistry, Vietnam Academy of Science and Technology (VAST), 18 Hoang Quoc Viet St., Cau Giay Dist., Ha Noi, Viet Nam*

[2]*Graduate University of Science and Technology, Vietnam Academy of Science and Technology (VAST), 18 Hoang Quoc Viet St.,, Cau Giay Dist.,, Ha Noi, Viet Nam*

[3]*Institute of Research and Development, Duy Tan University, 03 Quang Trung St., Da Nang, Viet Nam*

[4]*Faculty of Natural Sciences, Duy Tan University, 03 Quang Trung St., Da Nang, Viet Nam*

[*]Email: *daoduyquang@duytan.edu.vn*

Received: 24 May 2021; Accepted for Publication: 27 September 2021

Abstract. The surface-enhanced Raman scattering (SERS) phenomenon of 2,4,5-trichlorophenoxyacetic acid (2,4,5-T) adsorbed on Au_{20} pyramidal cluster is studied by Density Functional Theory. All possible adsorption configurations between the adsorbate and the Au_{20} clusters are evaluated and the vibrational assignments of normal Raman and SERS spectra are analyzed. The result shows that the most stable adsorption configuration of the adsorbate on Au_{20} cluster is formed by the interaction of O13 (-COOH group) and Au atom. The SERS activities of 2,4,5-T adsorbed on 1:1 Au-Ag and Au-Cu bimetallic clusters are also investigated. For bimetallic clusters, the substitution of 1, 4 or 10 Au atoms by Ag/Cu is performed by replacing the respective number of Ag/Cu atoms in 1, 2 and 3 parallel layers of the Au_{20} cluster. While the Raman scattering activity of the $Au_{10}Ag_{10}$ cluster is comparable to that of the Au_{20} cluster, it is remarkably higher than the $Au_{10}Cu_{10}$ cluster. This observation is explained by the molecule-to-cluster charge transfer process. The obtained results are hoped to contribute to better design of SERS-based analytical sensors for mobile and on-site applications.

Keywords: 2,4,5-T, herbicide, Raman, SERS, cluster, DFT.

Classification numbers: 2.1.1, 2.4.4, 3.2.1,

1. INTRODUCTION

2,4,5-trichlorophenoxyacetic acid (2,4,5-T) has been used as a chlorophenoxy herbicide to defoliate broad-leafed plants since the 1940s [1]. During the Viet Nam War (from 1961 to 1971), the Agent Orange, which is a mixture of two herbicides including 2,4,5-T and 2,4-D (2,4-dichlorophenoxyacetic acid) of equal portion and a trace amount of dioxin (TCDD, 2,3,7,8-

tetrachlorodibenzo-p-dioxin), was used by the US military as part of the herbicidal warfare program. This chemical has caused severe damage to the environment and serious health problems for many people who have been exposed to them. For example, the 2,4,5-T itself is toxic with a NOAEL (no-observed-adverse-effect level) of 3 mg/kg/day and a LOAEL (lowest-observed-adverse-effect level) of 10 mg/kg/day [2]. Although the effects of 2,4,5-T herbicide on human health at low environmental doses are not evident, intentional overdoses and unintentional high dose occupational exposures to the herbicide, especially after its use, have been reported to result in headache, dizziness, abdominal pain, renal and hepatic injury, and delayed neuropathy [3]. Other studies have reported the biological effects of 2,4,5-T with the presence of trace concentrations of TCDD [4]. Thus, the development of analytical sensors for qualitative and quantitative detection of 2,4,5-T herbicide accumulated in the environment or agricultural products is of interest for either experimental or computational works.

There are several analytical techniques to analyze a trace amount of a compound such as GC, MS, HPLC, Raman and FTIR. However, these techniques have a limit concerning their mobility in cases of on-site measurements for environmental monitoring purposes. In recent decades, Surface-Enhanced Raman Spectroscopy (SERS), which shows an enhanced Raman scattering signal when a molecule adsorbed on a rough coinage metal surface (i.e., silver, gold, and copper), has attracted great interest. Under ideal conditions, SERS could increase the Raman intensity of the molecules analyzed up to 10^6 times its normal Raman intensity [5]. However, unlike our expectations while searching for an appropriate herbicide detection method, there has scarcely been SERS studies on 2,4,5-T. Among very few examples, Karthikeyan *et al.* evaluated only the FT-IR, FT-Raman and NMR spectra of 2,4,5-T using experimental and density functional theory (DFT) approaches [6]. In this work, Raman characteristic frequencies of the 2,4,5-T compound are experimentally identified and their vibrations are elucidated using DFT calculations. Since the 2,4,5-T molecule contains three chlorine atoms at the 2, 4 and 5 positions on the aromatic ring, a Raman band with a strong intensity at 690 cm^{-1} was assigned to C−Cl stretching vibration. Similarly, several bands centered at 350, 290 and 280 cm^{-1} were determined for C−Cl in-plane bending modes and at 170, 150 and 120 cm^{-1} for C−Cl out-of-plane deformation vibrations. Other strong bands at 3080, 1595, 1140, 935 and 200 cm^{-1} were assigned to C−H ring stretching, C=C stretching, C−H in-plane bending, O−H out-of-plane bending, and C−O out-of-plane bending vibrations, respectively. To the best of our knowledge, there have been no experimental or computational studies on the analysis of 2,4,5-T herbicide using the SERS technique.

Thus, the main goal of this study is to analyze the Raman characteristic frequencies as well as the surface-enhanced Raman spectroscopy (SERS) properties of the 2,4,5-T molecule adsorbed on the pyramidal Au_{20} cluster. This model can be used to simulate Au nanoparticles (AuNPs) in comparison with experiments. The chemical influence of bimetallic clusters of Au/Ag and Au/Cu models on the SERS characteristic frequencies is also evaluated. The obtained data are expected to contribute to the design of new mobile sensors for on-site analytical purposes.

2. COMPUTATIONAL METHODS

All calculations were performed using Gaussian 16 Rev.A.03 package [7] employing the PBE [8, 9] density functional combined with the cc-pVDZ-PP basis set for the metallic elements and the cc-pVDZ one for the other elements. The PBE functional was successfully used to predict Raman and SERS spectra of chlorpyrifos [10] which has a similar molecular structure to the 2,4,5-T one. To represent the gold nanoparticles, we used the Au_{20} pyramidal cluster model.

The validity of this choice was proved in a recent study, in which the adsorption configurations of chlorpyrifos molecule on the Ag_{20} pyramidal cluster model were in good agreement with the ones on the extended Ag surfaces using periodic boundary conditions calculated by the Vienna *ab-initio* simulation package (VASP) [10]. The most stable configuration of the complex between the 2,4,5-T molecule and the Au_{20} cluster was found by evaluating the binding energy and Gibbs free energy of all possible configurations.

The binding energy (E_b) between the 2,4,5-T and an Au_{20} cluster was calculated based on equation (1)

$$E_b = E_{complex} - (E_{cluster} + E_{2,4,5\text{-}T}) \quad (1)$$

where E consisted of the sum of electronic and thermal energies for a species. A negative value of E_b indicated favorable adsorption of the 2,4,5-T on Au_{20} clusters.

The Gibbs free energies at 298 K of the adsorption process were predicted as in equation (2)

$$\Delta G_b\,(298) = G_{complex} - (G_{cluster} + G_{2,4,5\text{-}T}) \quad (2)$$

where G was the sum of electronic and thermal free energies of a species. The lower the ΔG value, the more favorable the adsorption process of 2,4,5-T on the clusters. The normal Raman and SERS spectra were visualized and their spectral data are exported using GaussView 6.1 software.

The influence of bimetallic clusters on the SERS spectra was observed when mixing one, two and three layers of Au atoms by Ag and Cu ones. The obtained SERS spectra were then compared to the ones of the pure clusters.

3. RESULTS AND DISCUSSION

3.1. Adsorption configurations of 2,4,5-T–Au_{20} complexes

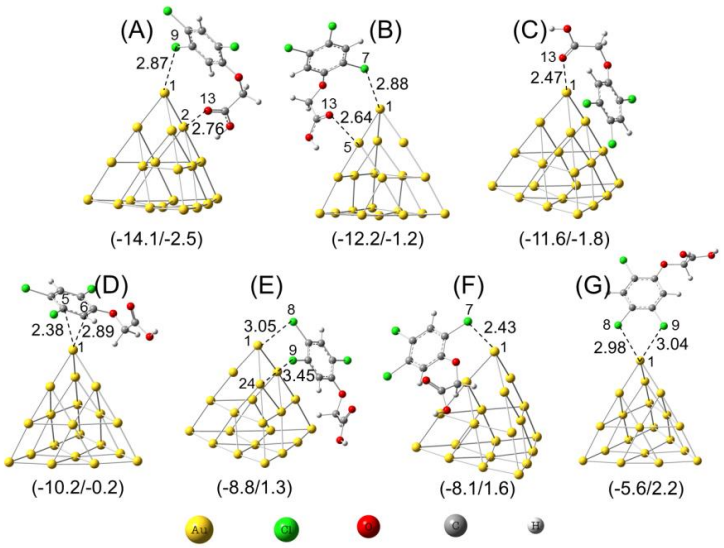

Figure 1. Optimized structure of the 2,4,5-T–Au_{20} complexes calculated at the PBE/cc-pVDZ-PP//cc-pVDZ level of theory. Bond distances are in Å and angles are in degree. Binding energies (E_b) and Gibbs energies (ΔG_b) of each configuration at 298 K are in parentheses and the unit is kcal/mol. Small grey, white, red and green balls represent carbon (C), hydrogen (H), oxygen (O), and chlorine (Cl) atoms, respectively, while big yellow balls represent gold atoms (Au).

Figure 1 represents all possible adsorption configurations between the 2,4,5-T with the Au_{20} cluster calculated in the gas phase at the PBE/cc-pVDZ-PP//cc-pVDZ level of theory. Cartesians coordinates of the studied 2,4,5-T-Au_{20} complexes are listed in Table S1 of the ESI file. As can be seen in Figure 1, the most stable adsorption configuration (**mode A**) is stabilized by two interactions between the adsorbate molecule and Au_{20} cluster, i.e., Cl9-Au1 and O13-Au2 interaction, with the distance of 2.87 and 2.76 Å, respectively, which may be assumed for van der Waals radii [11]. The binding energies (E_b) and Gibbs energies (ΔG_b) of **mode A** configuration are -14.1 and -2.5 kcal/mol. Two other configurations, which have the same kind of interactions Cl7-Au1 (2.88 Å, **mode B**), O13-Cl5 (2.64 Å, **mode B**), or O13-Au1 (2.47 Å, **mode C**), are slightly less energetic stable with a difference of only 1-2 kcal/mol. Besides, the interactions of the Au_{20} cluster with the aromatic ring as well as the sole Cl atoms are further less stable in terms of energy (**mode D-G**). It seems that the most stable adsorption configurations are related to the interaction between Au atom and O13 of the –COOH group. This observation is reasonable, considering that one of the most negatively charged areas of the 2,4,5-T molecule is found at the –C=O of –COOH group. Finally, the negative binding energies (E_b) of all the configurations, from -14.1 to -5.6 kcal/mol, indicate that all the complexes are stable at 298 K.

3.2. Raman and SERS spectra of 2,4,5-T and the 2,4,5-T–Au_{20} complex

Normal Raman spectra as well as SERS one obtained for the most stable adsorption configuration of 2,4,5-T-Au_{20} complex, i.e., mode A (Figure 1) are presented in Figure 2. Table 1 assigns the vibrational peak of both spectra in comparison with the previously reported data.

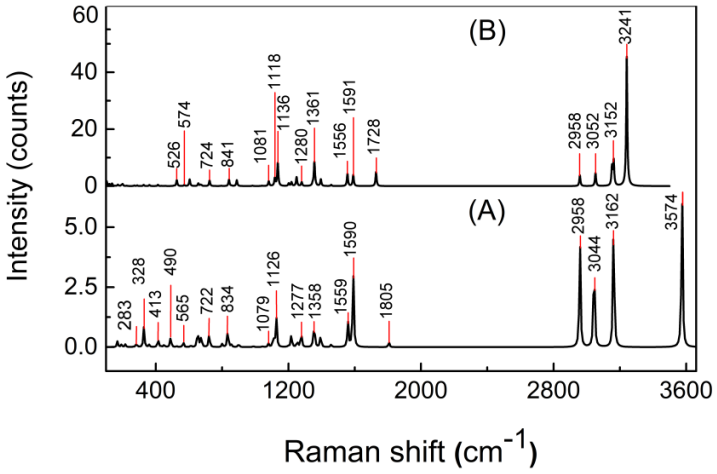

Figure 2. (**A**) Raman spectrum of 2,4,5-T and (**B**) SERS spectra of 2,4,5-T adsorbed on the Au_{20}cluster.

As can be seen in Figure 2 and Table 1, characteristic Raman peaks of the 2,4,5-T molecule are enhanced in SERS spectra when 2,4,5-T is adsorbed on the Au_{20} cluster. Indeed, the C=O symmetric stretching signal appeared at 1805 cm^{-1} on the normal Raman spectrum is shifted to 1728 cm^{-1} in SERS spectra but enhanced up to 23 times. The Raman intensities of this C=O stretching increased from 4 to 91 $Å^4$/amu. Moreover, the C=C ring stretching mode (1559 cm^{-1} in normal Raman and 1556 cm^{-1} in SERS) is enhanced four times with the Raman intensities from 19 to 76 $Å^4$/amu. Another significantly enhanced band with Raman activities increased 20 times from 7 to 140 $Å^4$/amu at 1358 cm^{-1} is the mixed O-H scissoring/CH_2 scissoring/ring stretching vibrations, the peak of which is 1358 and 1356 cm^{-1} in normal Raman and SERS, respectively. Similarly, the intensities of the peaks at 1126, 722 and 490 cm^{-1} are also enhanced

at 1136, 724 and 526 cm^{-1} which represent C-H in-plane rocking, C-Cl stretching and C-OOH twisting vibrations, respectively. The calculated Raman peaks are in good agreement with the one reported by Karthikeyan [6].

Table 1. Raman and SERS spectra of 2,4,5-T adsorbed on the Au_{20} cluster calculated at the PBE/cc-pVDZ-PP//cc-pVDZ level of theory in the gas phase. Raman scattering activities are given in parentheses in $Å^4$/amu, where amu stands for the atomic mass unit.

Raman		**SERS**	**Vibrational assignments**
This work	*Ref.* [6]		
3162 (158)	3080	3152 (169)	Ring C-H symmetric stretching
3044 (115)	-	3052 (118)	CH_2 asymmetric stretching
2958 (118)	2940	2958 (95)	CH_2 symmetric stretching
1805 (4)	-	1728 (91)	C = O symmetric stretching
1590 (61)	1595	1591 (70)	Ring C=C symmetric stretching
1559 (19)	-	1556 (76)	Ring C=C symmetric stretching
1458 (2)	1480	1458 (8)	Ring C=C symmetric stretching / Ring C-H wagging
1358 (7)	1350	1356 (140)	O-H scissoring/ CH_2 scissoring/Ring stretching
1277 (11)	1280	1280 (23)	CH_2 wagging and O-H scissoring/Ring breathing
1253 (4)	1260	1249 (23)	CH_2 wagging and O-H scissoring/Ring breathing
1218 (9)	-	1218 (22)	CH_2 twisting/ Ring breathing
1126 (21)	1140	1136 (130)	C-H in-plane rocking/O-H rocking
1079 (2)	1090	1081 (27)	Ring C-H wagging/O-H rocking
988 (1)	910	983 (2)	CH_2 rocking/C-C twisting
834 (12)	-	841 (34)	C-C stretching/O-H scissoring
801 (2)	760	794 (2)	Ring C-H out-plane bending
722 (8)	690	724 (29)	C-Cl stretching
565 (3)	550	571 (6)	Ring in-plane bending/ C-OOH scissoring
490 (6)	-	526 (30)	C-OOH twisting/ CH_2 rocking
413 (5)	440	413 (6)	C-O in-plane bending/ CH_2 rocking
328 (11)	350	327 (6)	C-Cl in-plane bending/ CH_2 rocking
283 (2)	280	288 (3)	C-Cl in-plane bending
264 (0.2)	200	270 (3)	C-O out-plane bending

3.3. SERS spectra of 2,4,5-T adsorbed on the Ag-Au and Cu-Au bimetallic clusters

In this section, we evaluate the influence of mixing 1, 2, 3 layers of Cu/Ag in the Au_{20} cluster on the SERS signal intensities. Recently, Truong *et al*. (2021) reported that the SERS intensities of Thiram pesticide adsorbed on the pure Cu_{20} pyramidal cluster are enhanced by 3 and 6 times compared with those obtained with Ag_{20} and Au_{20} clusters, respectively [12].

However, the copper nanoparticles are not typical for analysis sensors because of their easily oxidizable property in air, whereas Au and Ag metals are more stable or inert to oxidation. Thus, a question arises as to whether the mixed layer of Cu/Ag/Au NPs results in enhanced Raman signals while providing better oxidative stability. The obtained results may be interesting for SERS-based sensor designs. Figure 3 presents the SERS spectra obtained from the adsorption of the 2,4,5-T molecule on the mixed cluster in which 1, 4 and 10 Cu or Ag atoms arranged by 1, 2 and 3 parallel layers mixed into the Au_{20} cluster. Cartesians coordinates of the studied complexes are listed in Table S2 of the ESI file.

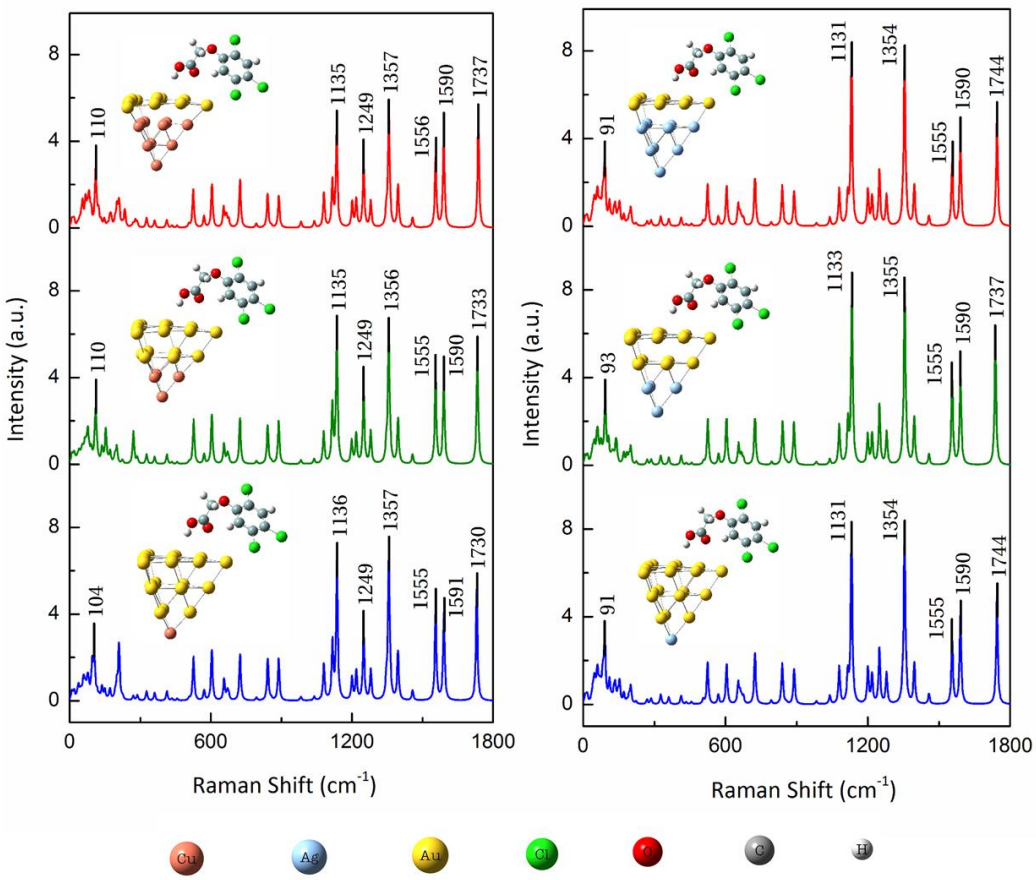

Figure 3. SERS spectra obtained from the adsorption of 2,4,5-T onto the pyramidal cluster M_{20} (M = Au, Ag or Cu) with different mixing configurations: (**a**) Cu_nAu_{20-n} clusters (n = 1, 4, 10); (**b**) Ag_nAu_{20-n} clusters (n = 1, 4, 10). Adsorption configuration consists of the most stable one obtained with the Au_{20} cluster. The optimized geometries of all the [2,4,5-T–M_{20}] complexes calculated at the PBE/cc-pVDZ-PP//cc-pVDZ level of theory in the gas phase are also shown above each spectrum. Small grey, white, red and green balls represent carbon (C), hydrogen (H), oxygen (O) and chlorine (Cl) atoms, respectively, while big yellow and orange balls represent gold (Au) and copper (Au) atoms, respectively.

As can be seen in Figure 3a, increasing the number of Cu atoms into the Au_{20} cluster slightly reduced the SERS intensities. For example, for the O-H scissoring vibration (1356 cm^{-1}), the Raman intensities decreased from 140 $Å^4$/amu (Au_{20} cluster) to 111, 98 and 82 $Å^4$/amu for the substitution of Au_{20} with 1, 4 and 10 Cu atoms, respectively. The same trend is also observed for the Ag-Au mixing configurations (Figure 3b).

Furthermore, regarding the nature of the bimetallic clusters to the enhancement factor in SERS spectra, it is noteworthy that the $Au_{10}Ag_{10}$ mixing mode (Figure 3b) represents better SERS activities than the $Au_{10}Cu_{10}$ one (Figure 3a). For example, the Raman activities of the 1357 cm^{-1} peak for the $Au_{10}Cu_{10}$ cluster are 82 $Å^4$/amu, and the ones of the 1354 cm^{-1} peak for $Au_{10}Ag_{10}$ cluster are 124 $Å^4$/amu, while the ones of the Au_{20} cluster are 140 $Å^4$/amu. Thus, the SERS activities obtained with the $Au_{10}Ag_{10}$ cluster are comparable with those from the pure Au_{20} cluster. This result proposes that a sensor using Ag NPs covered by an Au layer provides good SERS activities like the one using pure Au NPs, which is interesting in the SERS-based sensor applications in terms of reducing the price of commercial sensors.

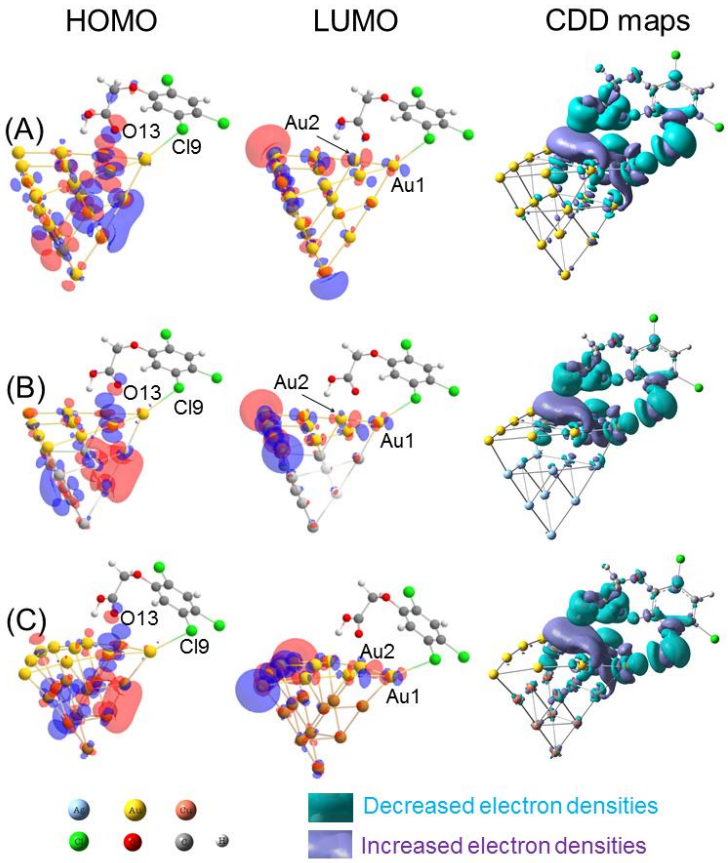

Figure 4. HOMO, LUMO distributions and charge density difference (CDD) maps of the most stable adsorption configurations between 2,4,5-T with (**A**) Au_{20} cluster (4 Au atom layers) and with the bimetallic cluster (**B**) $Au_{10}Ag_{10}$ and (**C**) $Au_{10}Cu_{10}$. The iso-value for CDD maps is 0.006.

In order to give insights into the influence of mixed clusters on SERS activity, Figure 4 displays the highest occupied molecular orbital (HOMO), lowest unoccupied molecular orbital (LUMO) distributions, and charge density difference (CDD) maps for the most stable adsorption configuration between the 2,4,5-T molecule with Au_{20}, $Au_{10}Ag_{10}$ and $Au_{10}Cu_{10}$ clusters. Figure 4 again confirms the charge transfer trend from the 2,4,5-T ligand to the cluster. In fact, all the HOMOs are equally distributed both on the ligand and the clusters, while the LUMOs show that the electron densities move entirely to the clusters. This observation is confirmed by CDD maps

where regions of decreased electron density are mostly found on the ligand side and regions of increased electron density are located on the cluster side.

To confirm the above observations, natural bond orbital (NBO) analysis was also performed in this study at the same level of theory. Table 2 presents meaningful donor and acceptor NBO interactions and their stabilization energies [E(2)] for the complexes of 2,4,5-T with Au_{20}, $Au_{10}Ag_{10}$ and $Au_{10}Cu_{10}$ clusters.

Table 2. Donor and acceptor NBO interactions and their stabilization energies [E(2)] for the complexes of 2,4,5-T with Au_{20}, $Au_{10}Ag_{10}$ and $Au_{10}Cu_{10}$ clusters. The numbering of atoms is based on Figure 4.

Complexes	Donor NBO (i)	Acceptor NBO (j)	E(2), kcal/mol
2,4,5-T–Au_{20}	LP(1) Cl9	LP*(7) Au1	16.2
	LP(3) Cl9	LP*(7) Au1	7.4
	LP(1) O13	LP*(8) Au2	12.0
2,4,5-T–$Au_{10}Ag_{10}$	LP(1) Cl9	LP*(7) Au1	15.9
	LP(2) Cl9	LP*(7) Au1	5.7
	LP(3) Cl9	LP (6) Au1	7.9
	LP(3) Cl9	LP*(7) Au1	6.6
	LP(1) O13	LP*(8) Au2	11.7
2,4,5-T–$Au_{10}Cu_{10}$	LP(1)Cl9	LP*(7) Au1	15.4
	LP(2)Cl9	LP*(7) Au1	4.6
	LP(3)Cl9	LP (6) Au1	8.0
	LP(3)Cl9	LP*(7) Au1	4.9
	LP(1) O13	LP*(8) Au2	12.7

As can be seen in Table 2, the adsorbate 2,4,5-T principally coordinates with the clusters *via* the interaction between the lone electron pair on the Cl9 and O13 atoms with the antibonding lone electrons pair on the Au1 and Au2 atoms. Indeed, for the [2,4,5-T–Au_{20}] complex the electron densities are transferred from LP(1) Cl9 to LP*(7) Au1 and from LP(1) O13 to LP*(8) Au2 with a stabilization energy [E(2)] of 16.2 and 12.0 kcal/mol, respectively. For the [2,4,5-T–$Au_{10}Ag_{10}$] complex, the electron densities are essentially shifted from the LP(1) Cl9 to the LP*(7) Au1 with an E(2) value of 15.9 kcal/mol, and from the LP(1) O13 to the LP*(8) Au2 with an E(2) value of 11.7 kcal/mol. Similarly, the electrons are also donated from the LP(1) Cl9 to the LP*(7) Au1 and from the LP(1) O13 to the LP*(8) Au2 with E(2) values of 15.4 and 12.7 kcal/mol, respectively for the [2,4,5-T–$Au_{10}Cu_{10}$] complex. The observation of the molecule-to-cluster charge transfer at the ground state is in good agreement with recent studies on thiram [12] and chlorpyrifos [10] pesticides.

Furthermore, we analyze the Hirshfeld atomic charges of different heavy atoms in the complexes between 2,4,5-T with $Au_{10}Cu_{10}$, $Au_{10}Ag_{10}$, and $Ag_{10}Au_{10}$ clusters as an example (**Table 3**). The total atomic charges of the 2,4,5-T ligand decrease from 0.053 e^- for adsorption on the Au_{20} cluster, to 0.035 e^- and 0.020 e^- for $Au_{10}Cu_{10}$ and $Au_{10}Ag_{10}$ clusters, respectively. In the isolated state, the 2,4,5-T molecule is neutral in charge, and thus when the studied molecule

adsorbed on the cluster, the molecule-to-cluster charge transfer (CT) occurs, leading to positive charges of the adsorbate. For that reason, the more positively charged the adsorbate, the more important the CT. Our results indicate that CT is decreased for the $Au_{10}Ag_{10}$ and $Au_{10}Cu_{10}$ clusters compared to the pure Au_{20} cluster. This observation is in line with the fact that the total charges of the contact layer on the surface (i.e., Au_{10} triangle surface) become more negative for the cases of the mixed clusters. In fact, the total charge of Au_{10} surface decreases from -0.027 e^- for Au_{20} to -0.181 and -0.163 e^- for $Au_{10}Ag_{10}$ and $Au_{10}Cu_{10}$ cluster, respectively. The contact surface in negative charge will not favor the reception of electron densities from the adsorbate molecule, and thus limit the CT process.

Table 3. Total Hirshfeld atomic charges with hydrogen atoms summed into heavy atoms for the 2,4,5-T adsorbate, the Au_{10} contact layer, and the Au_{10}, Ag_{10} and Cu_{10} three under layers in the Au_{20}, $Au_{10}Ag_{10}$ and $Au_{10}Cu_{10}$ clusters, respectively. All calculations are performed at the PBE/cc-pVDZ-PP//cc-pVDZ level of theory in the gas phase.

Total atomic charges	**Au_{20}**	**$Au_{10}Ag_{10}$**	**$Au_{10}Cu_{10}$**
2,4,5-T adsorbate	0.053	0.020	0.035
Au_{10} contact layers	-0.027	-0.181	-0.163
Au_{10} three base layers	-0.026	-	-
Ag_{10} three base layers	-	0.161	-
Cu_{10} three base layers	-	-	0.128

It has widely been accepted that the SERS chemical enhancement mechanism is related to the CT phenomena. Thus, the SERS enhancement is reduced from the Au_{20} to $Au_{10}Ag_{10}$ and $Au_{10}Cu_{10}$ clusters. This study highlights an observation of the reduced effect of SERS chemical enhancement by mixed Cu atoms in the Au_{20} cluster, which is reverse when compared with the results reported by Truong *et al.* [12].

4. CONCLUSIONS

SERS chemical enhancement of the herbicide 2,4,5-T by adsorption on the Au_{20} pyramidal cluster was evaluated by DFT using the PBE functional with the cc-pVDZ-PP basis set for the metallic atoms and the cc-pVDZ one for the other atoms. The possible interaction configurations between the adsorbate and the Au_{20} cluster were considered to reach the most stable structure. As a result, the most stable adsorption configurations are all formed by the interaction between the O13 atom of –COOH group with the Au atom on the top of the cluster. The binding energy and Gibbs energy of the most stable configuration are -14.1 and -2.5 kcal/mol, respectively. The effect of using bimetallic clusters, i.e. Ag-Au and Cu-Au on the Raman scattering activities were also investigated. The substitution of Ag and Cu atoms into the Au_{20} cluster slightly reduces the SERS activities, which may be due to the decrease of charge transfer from molecule to cluster. The SERS intensities obtained from the $Au_{10}Ag_{10}$ are found to be similar to that of the Au_{20} cluster and higher than that of the $Au_{10}Cu_{10}$ cluster. Although the layer-by-layer mixed clusters designed in this study do not result in the expected enhanced SERS intensities, the obtained results may be helpful for future works on the analysis sensor designs. Other mixing configurations should be considered to achieve SERS enhancement.

Acknowledgements. This research is funded by the Viet Nam National Foundation for Science and Technology Development (NAFOSTED) under grant number 103.03-2018.366. Le Thi Thuy Huong is funded by Vingroup Joint Stock Company and supported by the Domestic Master/Ph.D. Scholarship Program of Vingroup Innovation Foundation (VinIF), Vingroup Big Data Institute (VINBIGDATA), code VINIF.2020.ThS.106. The authors are also grateful to the Gridchem (www.seagrid.org) for providing computer resources using the Extreme Science and Engineering Discovery Environment (XSEDE) supported by the USA National Science Foundation grant number ACI-10535.

CRediT authorship contribution statement. Thi Thuy Huong Le, Dinh Hieu Truong: investigation, drafting manuscript. Thi Le Anh Nguyen, Thi Chinh Ngo, Pham Minh Quan: data analysis, editing manuscript. Duy Quang Dao: methodology, supervision and revising manuscript.

Declaration of competing interest. The authors declare that they have no known competing financial interests or personal relationships that could have appeared to influence the work reported in this paper.

REFERENCES

1. Hayashi S., Sano T., Suyama K., Itoh K. - 2,4-Dichlorophenoxyacetic acid (2,4-D)- and 2,4,5-trichlorophenoxyacetic acid (2,4,5-T)-degrading gene cluster in the soybean root-nodulating bacterium Bradyrhizobium elkanii USDA94, Microbiol. Res. **188–189** (2016) 62-71. https://doi.org/10.1016/j.micres.2016.04.014.
2. Sodhy P. - The US-Malaysian nexus: Themes in superpower-small state relations, Institute of Strategic and International Studies, Malaysia, 1991.
3. Horvath R. S. - Microbial co-metabolism and the degradation of organic compounds in nature, Bacteriol. Rev. **36** (1972) 146-155. https://pubmed.ncbi.nlm.nih.gov/4557166.
4. Gunther F. A. - Residue Reviews: Reviews of Environmental Contamination and Toxicology, Springer Science & Business Media, 1984.
5. Langer J., Jimenez de Aberasturi D., Aizpurua J., Alvarez-Puebla R. A., Auguié B., Baumberg J. J., Bazan G. C., Bell S. E. J., Boisen A., Brolo A. G., Choo J., Cialla-May D., Deckert V., Fabris L., Faulds K., García de Abajo F. J., Goodacre R., Graham D., Haes A. J., Haynes C. L., Huck C., Itoh T., Käll M., Kneipp J., Kotov N. A., Kuang H., Le Ru E. C., Lee H. K., Li J. F., Ling X. Y., Maier S. A., Mayerhöfer T., Moskovits M., Murakoshi K., Nam J. M., Nie S., Ozaki Y., Pastoriza-Santos I., Perez-Juste J., Popp J., Pucci A., Reich S., Ren B., Schatz G. C., Shegai T., Schlücker S., Tay L. L., Thomas K. G., Tian Z. Q., Van Duyne R. P., Vo-Dinh T., Wang Y., Willets K. A., Xu C., Xu H., Xu Y., Yamamoto Y. S., Zhao B., Liz-Marzán L. M. - Present and Future of Surface-Enhanced Raman Scattering, ACS Nano **14** (1) (2020) 28-117. https://doi.org/10.1021/acsnano.9b04224.
6. Karthikeyan N., Joseph Prince J., Ramalingam S., Periandy S. - Vibrational spectroscopic [FT-IR, FT-Raman] investigation on (2,4,5-Trichlorophenoxy) Acetic acid using computational [HF and DFT] analysis, Spectrochim. Acta Part A Mol. Biomol. Spectrosc. **124** (2014) 165-177. https://doi.org/10.1016/j.saa.2013.12.105.
7. Frisch M. J., Trucks G. W., Schlegel H. B., Scuseria G. E., Robb M. A., Cheeseman J. R., Scalmani G., Barone V., Petersson G. A., Nakatsuji H., Li X., Caricato M., Marenich A. V., Bloino J., Janesko B. G., Gomperts R., Mennucci B., Hratchian H.P., Ortiz J. V., Izmaylov A. F., Sonnenberg J. L., Williams-Young D., Ding F., Lipparini F., Egidi F., Goings J., Peng B., Petrone A., Henderson T., Ranasinghe D., Zakrzewski V.G., Gao J., Rega N., Zheng G., Liang W., Hada M., Ehara M., Toyota K., Fukuda R., Hasegawa J.,

Ishida M., Nakajima T., Honda Y., Kitao O., Nakai H., Vreven T., Throssell K., Montgomery Jr J. A., Peralta J. E., Ogliaro F., Bearpark M. J., Heyd J. J., Brothers E. N., Kudin K. N., Staroverov V. N., Keith T. A., Kobayashi R., Normand J., Raghavachari K., Rendell A.P., Burant J.C., Iyengar S.S., Tomasi J., Cossi M., Millam J. M., Klene M., Adamo C., Cammi R., Ochterski J. W., Martin R. L., Morokuma K., Farkas O., Foresman J. B., Fox D. J. - Gaussion 16 Rev. A.03 (2016).

8. Perdew J. P., Burke K., Ernzerhof M. - Generalized Gradient Approximation Made Simple, Phys. Rev. Lett. **77** (1996) 3865-3868. https://doi.org/10.1103 /PhysRevLett.77.3865.
9. Perdew J. P., Burke K., Ernzerhof M. - Errata: Generalized gradient approximation made simple, Phys. Rev. Lett. 78 (1997) 1396.
10. Ngo T.C., Trinh Q.T., Thi Thai An N., Tri N.N., Trung N.T., Truong D.H., Huy B.T., Nguyen M.T., Dao D.Q., SERS Spectra of the Pesticide Chlorpyrifos Adsorbed on Silver Nanosurface: The Ag_{20} Cluster Model, J. Phys. Chem. C. **124** (2020) 21702-21716. https://doi.org/10.1021/acs.jpcc.0c06078.
11. Rowland R.S., Taylor R., Intermolecular Nonbonded Contact Distances in Organic Crystal Structures: Comparison with Distances Expected from van der Waals Radii, J. Phys. Chem. **100** (1996) 7384-7391. https://doi.org/10.1021/jp953141+.
12. Truong D. H., Ngo T. C., Ai Nhung N. T., Quang D. ., Dao D. Q. - SERS chemical enhancement by copper - nanostructures: Theoretical study of Thiram pesticide adsorbed on Cu_{20} cluster, Vietnam J. Chem. **59** (2020) 159-166.